

# Photoconductivity and Photoelectromagnetic Effects in InSb†

S. W. KURNICK, A. J. STRAUSS, AND R. N. ZITTER  
Chicago, Midway Laboratories, Chicago, Illinois  
(Received April 30, 1954)

**P**HOTOCONDUCTIVE and photoelectromagnetic<sup>1-3</sup> responses have been observed at 300°K and 77°K in *p*-type samples of InSb which are intrinsic at room temperature. The data reported here were obtained in experiments on rectangular plates measuring  $0.028 \times 0.26 \times 1.0$  cm<sup>3</sup> with an effective impurity concentration of approximately  $7 \times 10^{15}$  acceptors/cm<sup>3</sup> (as determined by Hall measurements at 77°K) and with a resistivity of 0.015 ohm-cm at 300°K and 1.1 ohm-cm at 77°K. Samples were placed in a cryostat with a rocksalt window and mounted between the pole pieces of an electromagnet. Illumination of approximately 0.05 watt/cm<sup>2</sup>, chopped at 525 cps, was supplied by a Nernst glower with a brightness temperature of about 1600°C. The sample length, magnetic field, and illumination were mutually perpendicular. A bias voltage could be applied across the sample for photoconductivity measurements. At 300°K the sample was connected through a transformer with impedance ratio 1:1600 to a Hewlett Packard Model 450A amplifier and then to a Hewlett Packard Model 300A harmonic wave analyzer. For measurements at 77°K, the sample was connected directly to the amplifier and wave analyzer. The results are more directly interpreted in terms of  $i_s$ , the "short-circuit" current. To obtain  $i_s$  from the observed current  $i_o$ , the formula  $i_s = i_o R_s / R$  is employed, where  $R_s$  is the resistance of the illuminated portion of the sample and  $R$  is the total resistance in the circuit. In cases where magnetoresistance effects (large  $\mu B$ ) are important, the resistance must be evaluated at the appropriate value of magnetic field.

On the basis of the simple model given by Moss, the short-circuit current generated by the photoelectromagnetic (PEM) effect is given by

$$i_s = \frac{\eta Q e B \mu (D\tau)^{1/2}}{1 + \mu^2 B^2} L \quad (1)$$

where  $\eta$  is the quantum efficiency,  $Q$  the photon flux,  $e$  the electronic charge,  $B$  the magnetic flux density, and  $L$  the length of the illuminated portion of the sample;  $\mu$ ,  $D$ ,  $\tau$  are, respectively, the mobility, diffusion constant, and effective lifetime of the excited electrons produced by the illumination. Since the electron mobility in InSb is much higher than the hole mobility, the contribution of the excited holes to the photocurrent at low magnetic fields may be neglected. It should be noted that the factor  $1/(1 + \mu^2 B^2)$  does not appear in Moss' expression for the short-circuit current because Moss applied the expression to data for PbS where  $\mu B \ll 1$ .

Figures 1 and 2 show that the observed variation of  $i_s$  with  $B$  is in good agreement with Eq. (1). The curves in Fig. 1 were

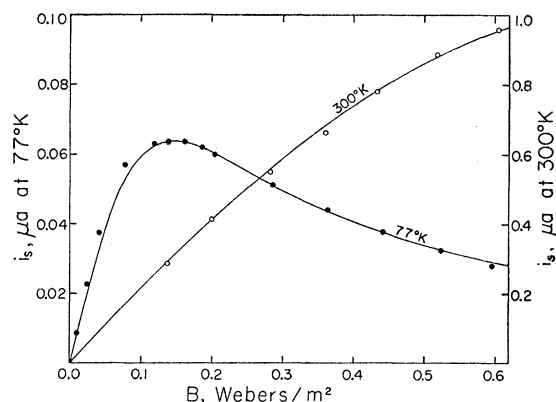


FIG. 1. PEM current versus magnetic flux density.

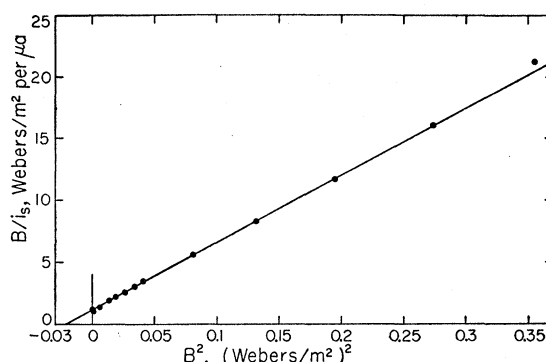


FIG. 2. Plot of  $B/i_s$  versus  $B^2$ .

calculated from the equation  $i_s = KB/(1 + \mu^2 B^2)$  using the values of  $K$  and  $\mu$  best fitting the experimental data. These parameters were found by plotting  $B/i_s$  versus  $B^2$  as shown in Fig. 2 for the results at 77°K. The mobilities found in this manner were 1.0 and 6.8 m<sup>2</sup>/v-sec at 300°K and 77°K, respectively. The former value is about one-fifth of the Hall mobility reported by Tanenbaum and Maita<sup>4</sup> for electrons in intrinsic single crystals at 300°K, while the latter is only about 10 percent less than the Hall mobility reported by these authors for electrons in an *n*-type single crystal. The value for 300°K agrees qualitatively with the electron mobility of 1.5 m<sup>2</sup>/v-sec derived from the magnetoresistance data of Pearson and Tanenbaum.<sup>5</sup>

Effective lifetimes estimated from the PEM data on the basis of Eq. (1), utilizing the derived mobilities, are about  $10^{-10}$  and  $10^{-13}$  sec at 300°K and 77°K, respectively. When lifetimes are derived from the photoconductive short-circuit current

$$i' = \eta Q e \mu F \tau / L \quad (2)$$

where  $F$  is the electric field, the values are  $10^{-8}$  and  $10^{-10}$  sec at 300°K and 77°K, respectively. The discrepancies between the photoconductive and PEM lifetimes may result at least in part from errors in the estimation of the photon flux  $Q$ . However, it seems unlikely that this is sufficient to account for all the inconsistencies since the ratio of photoconductive to PEM lifetime increases from  $10^2$  at 300°K to  $10^3$  at 77°K. Alternatively there may be real differences between the two effective lifetimes due to enhanced surface recombination in the magnetic field (Suhl effect).

† This research was supported in whole by the United States Air Force under a contract.

<sup>1</sup> Moss, Pincherle, and Woodward, Proc. Phys. Soc. (London) **B66**, 743 (1953).

<sup>2</sup> T. S. Moss, Proc. Phys. Soc. (London) **B66**, 993 (1953).

<sup>3</sup> P. Aigrain and H. Bulliard, Compt. rend. **236**, 595 and 672 (1953).

<sup>4</sup> M. Tanenbaum and J. P. Maita, Phys. Rev. **91**, 1009 (1953).

<sup>5</sup> G. L. Pearson and M. Tanenbaum, Phys. Rev. **90**, 153 (1953).

## Recombination of Holes and Electrons at Lineage Boundaries in Germanium

F. L. VOGEL, W. T. READ, AND L. C. LOVELL  
Bell Telephone Laboratories, Murray Hill, New Jersey  
(Received April 20, 1954)

**S**MALL-angle-of-misfit grain boundaries are made up of arrays of dislocations, which, in certain lineage boundaries in germanium, have been revealed by etch pits.<sup>1</sup> Dislocations in or near the edge orientation act like rows of closely spaced acceptor centers with energies slightly above the middle of the gap.<sup>2,3</sup> An occupied acceptor is a hole trap and an empty acceptor, an electron trap. Thus excess holes and electrons should recombine at a small-angle grain boundary made up of edge dislocations, and the boundary should have a characteristic recombination velocity. This letter describes some studies of recombination at grain boundaries in germanium. The dislocations, which are parallel

TABLE I. Boundary recombination velocities for several specimens.

Spec. no.	Resistivity, $\rho$ ohm-cm	Body lifetime, $\tau$ $\mu$ sec	Crystal boundary recombination velocity, $v$ cm/sec
A	16 — $n$	1100	$2.0 \times 10^3$
B	9.0 — $n$	450	1.2
C	7.1 — $n$	310	2.6
D	3.0 — $p$	250	1.6

and in the edge orientation, are spaced at intervals of about a micron.

The recombination was studied by the Morton-Haynes<sup>4</sup> method, illustrated in Fig. 1(a). The (movable) light source generates excess carriers and their concentration is measured as a function of the position  $x_l$  of the light source. In an  $n$ -type specimen the excess hole concentration at the (fixed) collector point is proportional to the collector current which is measured as the voltage,  $V$ , across a resistor in series with the collector. The straight-line portion of the  $V$  vs  $x_l$  plot gives body lifetime. Figure 1(b) shows  $V$  vs  $x_l$  for a fixed position,  $x_b$ , of the grain boundary. As the light approaches the grain boundary, the slope of the  $V$  vs  $x_l$  curve becomes steeper—indicating that the boundary is a sink for holes; that is, a greater fraction of the light-generated holes moves to the right, or toward the boundary, rather than to the left, or toward the collector.

At the top in Fig. 1(a) are the solutions to the diffusion equation giving the excess hole concentration  $\delta p(x)$  in the three regions shown. The bulk diffusion length is taken as unit length.  $A_1$ ,  $A_2$ ,  $B_2$ ,  $B_3$  are functions of  $x_l$  and  $x_b$ , and are determined by the following boundary conditions:  $\delta p(x)$  is continuous at  $x_l$  and  $x_b$ ; the discontinuity in hole current at  $x_l$  is the rate of hole generation and the discontinuity at  $x_b$  is  $v\delta p(x_b)$ , where  $v$  is the recombination velocity. Using the fact that  $\delta p$  at the collector ( $x=0$ ) is proportional to  $V$ , we find

$$\ln[1 - (V/V_0)] + \ln[(2v_1/v) + 1] = -2(x_b - x_l),$$

where  $V_0$  is the potential that would be observed in the absence of the grain boundary and  $v_1 = (\text{diffusion length})/(\text{lifetime})$  in the bulk material. When the light is 40 or more mils to the left of the

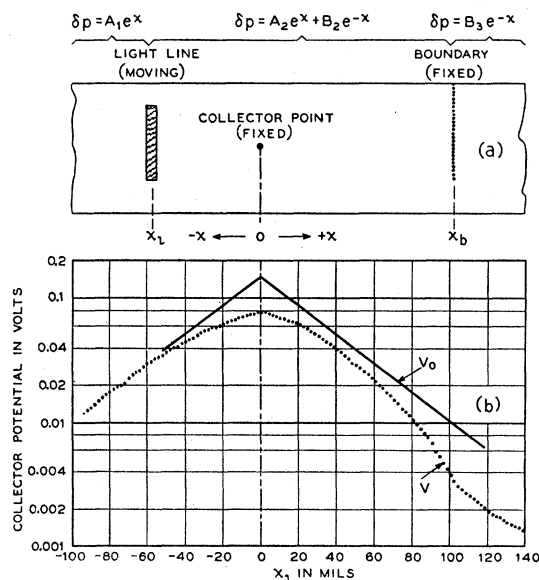


FIG. 1 (a) Diagram of the positions of the fixed collector point and grain boundary and the movable light line on an  $n$ -type specimen. At the top of the figure are the solutions of the diffusion equation for excess hole concentration  $\delta p$  vs distance  $x$  from the collector in the three regions indicated. (b) The collector potential plotted as a function of the position  $x_l$  of the movable light line for specimen B.

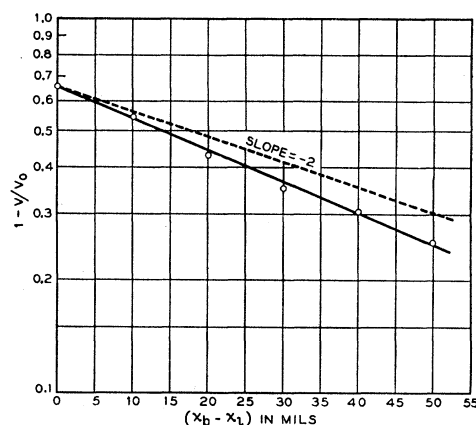


FIG. 2. Plot of  $1 - (V/V_0)$  versus  $(x_b - x_l)$ , where  $V$  is collector potential and  $V_0$  is the potential that would be observed in the absence of a grain boundary. Both  $V$  and  $V_0$  are found from Fig. 1(b). The theory predicts a straight line of slope  $-2$ .

collector, the points in Fig. 1(b) fall on a straight line, which reflected about  $x=0$  gives  $V_0$  for corresponding positions of the light to the right of the collector. Figure 2 shows a semilog plot of  $[1 - (V/V_0)]$  vs  $(x_b - x_l)$ . The points are well fitted by a straight line of slope  $-2$ . The intercept at  $x_b - x_l = 0$  gives  $v$ . Comparable agreement with the theory was obtained for three other specimens. Table I gives the resistivity, conductivity type, lifetime, and recombination velocity for the four specimens.

The existence of a surface recombination velocity at the crystal boundary indicates a concentration of recombination centers in the boundary. The density of these centers cannot, however, be calculated from the data because of uncertainties in (1) the carrier concentration in the space-charge region at the boundary, (2) the capture cross section, and (3) the number of traps which are charged.

<sup>1</sup> Vogel, Pfann, Corey, and Thomas, Phys. Rev. **90**, 489–489 (1953).

<sup>2</sup> W. Shockley, Phys. Rev. **91**, 228 (1953).

<sup>3</sup> Pearson, Read, and Morin, Phys. Rev. **93**, 666 (1954).

<sup>4</sup> L. B. Valdes, Proc. Inst. Radio Engrs. **40**, 1420 (1952).

## Magnetic Anisotropy of NiF<sub>2</sub>

L. M. MATARRESE AND J. W. STOUT

Institute for the Study of Metals and Department of Chemistry,  
The University of Chicago, Chicago, Illinois

(Received April 26, 1954)

IN an investigation of the magnetic anisotropy of a single crystal of NiF<sub>2</sub> we have observed phenomena which are unlike those found<sup>1,2</sup> in the isomorphous substances MnF<sub>2</sub>, FeF<sub>2</sub>, and CoF<sub>2</sub>, and which lead us to believe that below the Curie temperature a small ferromagnetic moment appears in NiF<sub>2</sub>. In a normal paramagnetic or antiferromagnetic substance the magnetic susceptibility may be represented by a second-order tensor and in this case the torque on a single crystal in a uniform magnetic field is proportional to the square of the field strength and to the sine of twice the angle between the field direction and the direction of maximum susceptibility in the plane of rotation. Such a behavior was observed for NiF<sub>2</sub> at temperatures above the maximum in heat capacity<sup>3</sup> occurring at 73.2°K. The single crystal was oriented so that the plane of rotation contained the tetragonal [001] axis and a [110] direction. Unlike the other isomorphous fluorides, the susceptibility of NiF<sub>2</sub> at room temperature was greater perpendicular to the tetragonal axis than parallel to it and the difference between the perpendicular and parallel molar susceptibilities rose gradually from  $1.102 \times 10^{-4}$  at 301.15°K to  $1.890 \times 10^{-4}$  at 90.07°K. Below 73.2°K the observed torques were large and anomalous in their dependence on field strength and angle. The torque measured